JOURNAL OF PHARMACEUTICAL SCIENCES

JULY 1984
VOLUME 73 NUMBER 7

RESEARCH ARTICLES

Pharmacokinetics of Capacity-Limited Tissue Distribution of Methicillin in Rabbits

FRANCIS M. GENGO *‡x, JEROME J. SCHENTAG‡, and WILLIAM J. JUSKO

Received December 8, 1982, from the *Departments of Pharmaceutics and Pharmacy, School of Pharmacy, State University of New York at Buffalo and ‡The Clinical Pharmacokinetics Laboratory, Millard Fillmore Hospital, Buffalo, NY 14209. Accepted for publication April 21, 1983.

Abstract □ Single-dose and steady-state studies were carried out in rabbits to characterize the pharmacokinetics of methicillin elimination and tissue distribution. Serum methicillin concentrations after single doses exhibited a biexponential decline with a mean terminal half-life of 27 ± 5 min. Steady-state volume of distribution (Vd_{ss}) decreased twofold as doses increased from 5 to 125 mg/kg, while total clearance was consistent over this dosage range. During steady-state infusions of 8.7–87.2 mg/kg/h, the serum and extravascular fluid concentrations increased in proportion to dose, while clearance remained constant. Methicillin tissue concentrations did not increase in proportion to dose and serum concentration, and the Vd_{ss} measured from tissue recovery decreased as dosage and serum concentrations increased. Central compartment volume and serum protein binding did not change. The cause of the dose-dependent change in Vd_{ss} was a capacity-limited uptake of methicillin into essentially all nonexcretory tissues. This process was described by a partial physiological pharmacokinetic model based on the actual weights or volumes of the rabbit tissues. Distribution into extracellular fluids was assumed to be complete, while entry into cellular, nonexcretory tissue became capacity limited as the K_m (17.2 μg/mL) was exceeded. The result was a decline in Vd_{ss} with increasing serum concentrations to a limiting value which approached the volume of the central space (V_c) and was similar to the extracellular water volume of the rabbit (0.17 L/kg). In the dosage range where total clearance was independent of serum concentration, the distribution of methicillin was concentration dependent and could be predicted by equations derived from the Michaelis–Menten equation.

Keyphrases □ Methicillin—pharmacokinetics in the rabbit, capacity-limited tissue distribution, single-dose and steady-state conditions □ Pharmacokinetics—methicillin in the rabbit, capacity-limited tissue distribution, single-dose and steady-state conditions □ Tissue distribution—capacity limited, methicillin, rabbits, pharmacokinetics, single-dose and steady-state conditions

Nonlinear disposition of drugs commonly occurs as a result of saturation in transformation, transport, or binding with or by biological substrates. Processes that are most frequently nonlinear are the enzyme-mediated active biotransformations of compounds, such as the metabolism of salicylates, ethanol, and phenytoin (1). Renal tubular secretory mechanisms of compounds such as *p*-aminohippuric acid are capacity limited (2), while tubular reabsorption of at least two cephalosporins is also a nonlinear process (3). Some radiocontrast agents such as iodipamide undergo apparent Michaelis–Menten-type biliary excretion in dogs (4). The GI absorption of some penicillins appear to be zero-order or capacity limited (5). Transport between CSF and blood is often active, as demonstrated for benzylpenicillin (6), but a generalized nonlinear tissue distribution pattern has not been reported for penicillins or any other drugs. If protein binding sites can be saturated to produce nonlinear kinetics, there is no reason why the same process cannot occur in the tissues (7). As an example of capacity-limited tissue binding, DiSanto and Wagner (8) have proposed a nonlinear tissue binding model to account for methylene blue distribution. Saturable or nonlinear plasma protein binding can have diverse effects on both drug distribution and clearance as evidenced with prednisolone (9).

The purpose of this report is to provide a pharmacokinetic description of methicillin serum and tissue concentrations in rabbits. The model incorporates capacity-limited transfer between extravascular fluid and tissues, and utilizes and tests transit time concepts to convert between single-dose and steady-state conditions.

THEORETICAL SECTION

Saturable tissue uptake and linear plasma clearance are the fundamental mechanisms proposed to describe the pharmacokinetics of methicillin over most of the dosage range of interest. A minimal model which describes the experimental data is shown in Fig. 1. The plasma and interstitial fluid comprise the central compartment (V_c), while remaining body tissues were considered as V_T. Total clearance, or the systemic plasma clearance of the drug (CL), occurs from the central compartment. Methicillin uptake into cellular spaces (CL_{12}) was nonlinear and Michaelis–Menten kinetics (T_{max}, K_m) were used to describe the rate-limiting mechanism. Return of drug from tissue to plasma (CL_{21}) was assumed to be linear.

0022-3549/84/0700-0867$01.00/0

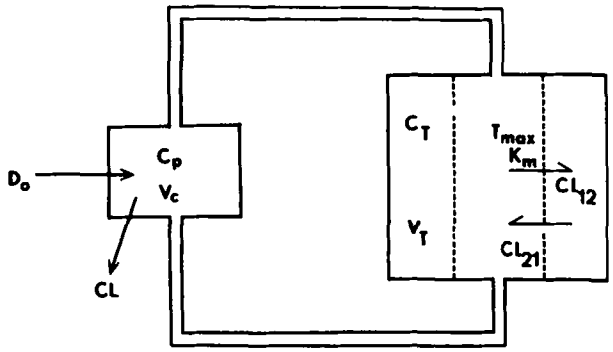

Figure 1—*Partial physiological model for methicillin distribution and clearance in the rabbit. The central volume (V_c) is assumed to comprise plasma and interstitial fluid, from which systemic clearance (CL) occurs. Remaining body tissues (V_T) attain drug concentrations (C_T) by nonlinear transport clearance [$CL_{12} = f(T_{max}, K_m)$] and linear distribution clearance (CL_{21}).*

The differential equations which describe serum (C) and overall tissue (C_T) concentrations are:

$$V_c \frac{dC}{dt} = -CL \cdot C - C \cdot CL_{12} + CL_{21} \cdot C_T \qquad \text{(Eq. 1)}$$

$$V_T \frac{dC_T}{dt} = CL_{12} \cdot C - CL_{21} \cdot C_T \qquad \text{(Eq. 2)}$$

where:

$$CL_{12} = \frac{T_{max}}{K_m + C} \qquad \text{(Eq. 3)}$$

reflects the nonlinear nature of tissue uptake of the drug. Unlike a perfusion model, where the concentration of drug in venous blood should be used in Eq. 2, V_T and C_T are employed here as the actual tissue (cellular) volumes and concentrations (excluding plasma and interstitial fluid). Equilibration between plasma and interstitial fluid was assumed to be very rapid in comparison with the rates of tissue uptake, and cellular transport or binding was considered to be the only mechanism for tissue uptake and retention. The nonlinearity of Eq. 3 prevents direct integration of these equations, but some of the model parameters can be estimated under initial, time-average, low-dose, and steady-state conditions.

Single-Dose Conditions—Serum concentrations following single intravenous bolus injections declined in a biexponential manner and were initially described by their SHAM (slope, height, area, moment) characteristics (10) with:

$$C = C_1^{-\lambda_1 t} + C_2^{-\lambda_2 t} \qquad \text{(Eq. 4)}$$

where C_i are intercepts and λ_i are slope values. These coefficients yield the total area (AUC) and first moment (AUMC) of each curve from:

$$\text{AUC} = \sum C_i/\lambda_i \qquad \text{(Eq. 5)}$$

$$\text{AUMC} = \sum \frac{C_i}{\lambda_i^2} \qquad \text{(Eq. 6)}$$

This permits calculation of mean transit time ($\bar{t}$) for each dose as:

$$\bar{t} = \text{AUMC}/\text{AUC} \qquad \text{(Eq. 7)}$$

The total plasma clearance of a drug is independent of distribution parameters (except for blood flow to the eliminating organ) and can be calculated from:

$$CL = \frac{D_0}{\text{AUC}} \qquad \text{(Eq. 8)}$$

where D_0 is the intravenous bolus dose. The volume of distribution at steady state (Vd_{ss}) can be obtained (11) as:

$$Vd_{ss} = CL \cdot \bar{t} \qquad \text{(Eq. 9)}$$

This parameter is generated initially as a time-average parameter, and its meaning and limitations will be described in more detail below. The volume of the central compartment is calculated from:

$$V_c = D_0/\sum C_i \qquad \text{(Eq. 10)}$$

If very small intravenous doses are used, the system operates under linear conditions, thus collapsing to the conventional two-compartment model within the context of this treatment. This permits the slope/intercept values to be defined as (7):

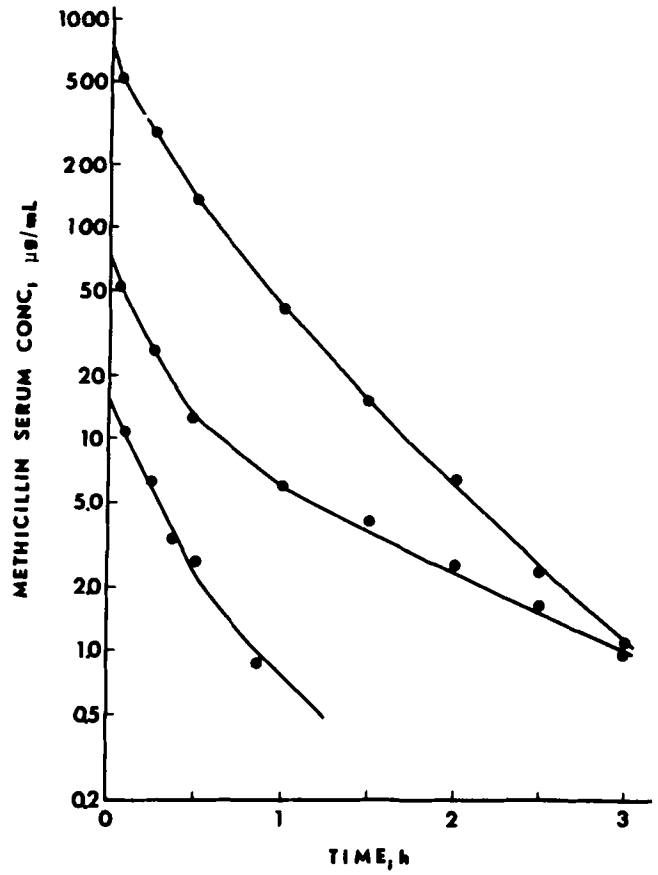

Figure 2—*Concentration-time course of 15-, 50-, and 500-mg/kg iv doses of methicillin in three different rabbits.*

$$\lambda_1 + \lambda_2 = CL/V_c + CL_{12}/V_c + CL_{21}/V_T = -b \qquad \text{(Eq. 11a)}$$

$$\lambda_1\lambda_2 = \frac{CL_{21} \cdot CL}{V_c \cdot V_T} = c \qquad \text{(Eq. 11b)}$$

$$\lambda_1,\lambda_2 = \frac{(-b \pm \sqrt{b^2 - 4c})}{2} \qquad \text{(Eq. 12)}$$

$$C_1 = \frac{D_0\left(\frac{CL_{21}}{V_T} - \lambda_1\right)}{V_c(\lambda_2 - \lambda_1)} \qquad \text{(Eq. 13)}$$

$$C_2 = \frac{D_0\left(\frac{CL_{21}}{V_T} - \lambda_2\right)}{V_c(\lambda_1 - \lambda_2)} \qquad \text{(Eq. 14)}$$

Estimates of the primary model parameters can be obtained, since CL, V_c, and Vd_{ss} are already solved. It is initially assumed (and will be demonstrated) that V_c and V_T have physiological meaning and represent the extracellular water and remaining body spaces of the animal. Thus:

$$V_T = \text{TBW}_t - V_c \qquad \text{(Eq. 15)}$$

where TBW_t is the total body weight of the animal. For convenience, these equations assume a body density of one, and thus body weight and volume are considered equivalent. From Eq. 11b we obtain:

$$CL_{21} = \frac{\lambda_1\lambda_2 \cdot V_c \cdot V_T}{CL} \qquad \text{(Eq. 16)}$$

thus providing CL_{12} from rearrangement of Eq. 11a:

$$CL_{12} = V_c(\lambda_1 + \lambda_2 - CL/V_c - CL_{21}/V_T \qquad \text{(Eq. 17)}$$

Alternatively, since (see below):

$$Vd_{ss} = V_c + \frac{CL_{12} \cdot V_T}{CL_{21}} \qquad \text{(Eq. 18)}$$

Table I—Time-Average Pharmacokinetic Parameters of Methicillin in Rabbits Following Single Intravenous Bolus Doses

Rabbit	Dose, mg/kg	CL, L/h/kg[a]	$\bar{t}$, h[b]	C_{av}, μg/mL[c]	Vd_{ss}, L/kg[d]	V_c, L/kg[e]	CL_{12}, L/h/kg[f]	CL_{21}, L/h/kg[g]
1	5.0	0.91	0.53	10.3	0.48	0.28	0.363	1.09
2	10.9	0.87	0.36	34.7	0.33	0.25	0.250	2.39
3	13.5	0.50	0.80	34.3	0.40	0.18	0.238	1.27
4	13.5	0.55	0.41	47.5	0.32	0.20	0.356	1.35
5	15.0	0.58	0.62	39.5	0.35	0.24	0.218	2.17
6	15.0	0.43	0.67	51.5	0.30	0.18	0.248	1.79
7	18.0	0.40	0.83	57.8	0.31	0.18	0.266	1.68
8	22.5	0.82	0.36	76.9	0.30	0.18	0.305	2.08
9	30.0	0.56	0.40	134.2	0.22	0.17	0.139	2.28
10	36.0	0.57	0.40	154.4	0.23	0.17	0.052	2.43
11	82.5	0.50	0.45	368.7	0.22	0.17	0.100	2.08
12	83.3	0.67	0.38	321.0	0.25	0.24	0.022	1.53
13	113.5	0.60	0.38	491.0	0.23	0.19	0.130	2.62
14	120.0	0.55	0.44	495.4	0.24	0.19	0.083	2.37
15	125.0	0.54	0.40	577.5	0.21	0.17	0.100	2.39

[a] Eq. 8. [b] Eq. 7. [c] Eq. 31. [d] Eq. 9. [e] Eq. 10. [f] Eq. 17. [g] Eq. 16.

a more direct solution is:

$$CL_{12} = \frac{CL_{21} \cdot (Vd_{ss} - V_c)}{V_T} \quad \text{(Eq. 19)}$$

Both Vd_{ss} and CL_{12} are time-average parameters when calculated in this manner and must be used cautiously when nonlinear conditions exist.

Steady-State Conditions—Ordinarily, the only pharmacokinetic parameter that can be obtained at steady state is the total clearance (CL). This value is usually calculated from the infusion rate (k_0) and the steady-state serum concentration (C^{ss}) as:

$$CL = k_0/C^{ss} \quad \text{(Eq. 20)}$$

However, the analysis and recovery of total body drug content (X_B^{ss}) also yields a direct value of Vd_{ss} from:

$$Vd_{ss} = X_B^{ss}/C^{ss} \quad \text{(Eq. 21)}$$

The conventional definition of Vd_{ss} is:

$$Vd_{ss} = V_c + \sum K_{pi} \cdot V_{ti} \quad \text{(Eq. 22)}$$

where K_{pi} and V_{ti} represent the partition coefficients and actual tissue weights or volumes for either the nonplasma or noncentral spaces of the body. In whole body terms, this can be written as:

$$Vd_{ss} = V_c + K_d \cdot \sum V_{ti} = V_c + (K_d \cdot V_T) \quad \text{(Eq. 23)}$$

where K_d is the overall tissue–serum distribution ratio. For the present model, K_d can be solved by considering steady-state conditions with Eq. 2 set to zero, yielding:

$$K_d = C_T^{ss}/C^{ss} = CL_{12}/CL_{21} \quad \text{(Eq. 24)}$$

or:

$$K_d = \frac{T_{max}}{CL_{21}(K_m + C^{ss})} \quad \text{(Eq. 25)}$$

or:

$$Vd_{ss} = V_c + \frac{T_{max} \cdot V_T}{(K_m + C^{ss})CL_{21}} \quad \text{(Eq. 26)}$$

With appropriate data, the unknown parameters of Eq. 26 can be solved by nonlinear least-squares iteration. To assist in resolution of such parameters, consider that as C^{ss} becomes very large ($C^{ss} \gg K_m$), the limiting value of Vd_{ss} is:

$$\lim_{C^{ss} \to \infty} Vd_{ss} = V_c \quad \text{(Eq. 27)}$$

At very low serum concentrations where linear distribution applies ($C^{ss} < K_m$):

$$\lim_{C^{ss} \to 0} Vd_{ss} = V_c + \frac{T_{max}V_T}{K_m \cdot CL_{21}} \quad \text{(Eq. 28)}$$

A typical Michaelis-Menten function usually has sufficient degrees of freedom to solve only two parameters. Equation 26 contains five parameters. In the present study, the single-dose experiments and large-dose infusions yield values of V_c (Eqs. 10 and 27). Retaining physiological equivalence for V_T permits its calculation from Eq. 15. The upper limit of CL_{12} (the quotient of T_{max}/K_m) and CL_{21} can be generated from single low-dose data (Eqs. 16 and 19). This leaves one unknown parameter. If Eq. 26 is rearranged to:

$$G = CL_{21} \cdot \frac{Vd_{ss} - V_c}{V_T} = \frac{T_{max}}{K_m + C^{ss}} \quad \text{(Eq. 29)}$$

then, the function G *versus* C^{ss} can be cast into linear form:

$$1/G = K_m/T_{max} + C^{ss}/T_{max} \quad \text{(Eq. 30)}$$

where a graph of $1/G$ *versus* C^{ss} yields a slope of $1/T_{max}$ and the ordinate intercept is K_m/T_{max}. However, by this stage the function G contains several inserted parameters and may be inaccurate. Thus, Eq. 30 is most useful for obtaining initial estimates. This allows the least-squares values of CL_{21}, T_{max}, and K_m to be generated by NONLIN curve-fitting of Eq. 26, using individual values of V_c and V_T from each animal and Vd_{ss} and C^{ss} as the dependent and independent variables. Because an array of T_{max} and CL_{21} values would yield an identical Vd_{ss} in Eq. 26, it is important to obtain reasonable parameter estimates to initiate computer fitting and to restrict the upper limit of T_{max}/K_m to CL_{12} as generated from the low-dose data (Eq. 3).

Single-Dose to Steady-State Conversion—For drugs with linear pharmacokinetic properties, any single-dose parameters apply directly to the steady-state situation. For drugs with nonlinear CL or Vd_{ss}, the parameters generated using Eqs. 8 and 9 were obtained as time-average values and must be considered valid only for the corresponding time-average serum concentration C_{av}. This is easily calculated as:

$$C_{av} = \text{AUC}/\bar{t} \quad \text{(Eq. 31)}$$

Thus, the equivalence between single-dose and steady-state conditions can be described as:

$$CL = \frac{k_0}{C_{av} \text{ or } C^{ss}} \quad \text{(Eq. 32)}$$

and:

$$Vd_{ss} = \frac{X_B^{ss}}{C^{ss}} = \frac{D_0}{C_{av}} \quad \text{(Eq. 33)}$$

These concepts are experimentally tested in this report.

EXPERIMENTAL SECTION

Protocol—A total of 31 male New Zealand White rabbits ranging in weight from 2.5 to 5.5 kg were studied. Fifteen animals were given single, rapid intravenous bolus doses of methicillin ranging from 5.0 to 125.0 mg/kg. Blood samples were collected from the marginal ear vein over the following 7 h.

Another group of 11 rabbits were given methicillin by constant infusion through a jugular vein catheter. Dosages ranged from 8.6 to 87.2 mg/kg/h, and infusion times ranged from 6.5 to 10 h. Cumulative total urine was collected from all of the animals over the next 24-h period, or until sacrifice. Five additional rabbits (2.5–2.7 kg) were each given a 15-, 50-, and 500-mg/kg bolus dose on different days in random sequence. Blood samples were collected from the marginal ear vein.

For collection of extravascular fluid, 5 of the 31 rabbits had perforated plastic balls (17-mL capacity) placed subcutaneously at 10–14 d prior to the methicillin infusion. In the other rabbits, peritoneal fluid was collected at sacrifice in a capillary tube or onto filter disks. The preweighed filter disks were placed in the abdominal cavity immediately after the animals were

Table II—Steady-State Pharmacokinetic Parameters of Methicillin in Rabbits Following Constant-Infusion Dosing

Rabbit	Weight, kg	Infusion Rate, mg/kg/h	CL, L/h/kg[a]	C^{ss}, μg/mL	Vd_{ss}, L/kg[b]	X_B^{ss}, mg
16	3.3	8.7	0.67	13.0	0.43	18.9
17	3.1	17.8	1.30	15.0	0.49	25.0
18	4.0	16.8	0.96	17.4	0.53	36.2
19	3.3	19.8	0.88	22.5	0.48	36.4
20	3.1	33.3	1.08	30.7	0.36	37.8
21	3.5	22.1	0.64	34.5	0.40	46.3
22	3.1	30.9	0.81	38.5	0.29	35.7
23	2.5	58.5	0.99	58.9	0.17	25.2
24	3.5	50.6	0.84	60.0	0.26	53.4
25	3.3	53.8	0.75	71.0	0.27	64.6
26	3.2	87.2	0.69	125.0	0.25	100.0

[a] Eq. 20. [b] Eq. 21.

sacrificed. Fluid in the abdominal cavity was tested for occult blood[1]; only negative samples were used for analysis.

At the end of the sampling procedures, all rabbits given continuous infusion were sacrificed, and samples of essentially all organs and tissues were obtained for methicillin assay. Urine was collected from the intact bladder. All organs and the remaining carcass were weighed for use in determining the organ content of methicillin.

Assays—Methicillin concentrations in serum, peritoneal fluid, and urine were determined by an agar well diffusion microbiological assay as outlined by Kavanaugh (12) using *Bacillus subtilis* as the test organism. The range of concentrations assayed without dilution was 0.5–25.0 μg/mL, and the day-to-day coefficient of variation was <10%. Samples were assayed in triplicate on two or more occasions and quantitated in reference to appropriate standards prepared in blank tissue homogenate, urine, or pooled rabbit serum. Plasma protein binding was measured by equilibrium dialysis at 37°C.

Tissue concentrations were determined by methods similar to those used previously (13). Necropsy samples were blotted on gauze and two 100–200-mg samples were weighed to be within 10 mg of each other. Each sample was individually homogenized following the addition of 1–2 mL of phosphate buffer (pH 7.4). To one of the two samples, a known amount of methicillin was also added. Samples were allowed to stand for 24–48 h at 4°C and then centrifuged. The supernatant was assayed using the microbiological assay and homogenate standards. The phosphate buffer in the homogenized tissue was replaced, and the extraction procedure was repeated until no further methicillin could be measured.

Extraction recovery was calculated using the following:

$$\frac{\begin{pmatrix}\text{Methicillin recovered}\\ \text{from "spiked" sample}\end{pmatrix} - \begin{pmatrix}\text{Methicillin recovered}\\ \text{from "unspiked" sample}\end{pmatrix}}{\text{Amount of Methicillin "spiked"}} \quad \text{(Eq. 34)}$$

The fractional extraction recovery using this method ranged from 0.9 to 1.05 in all tissues.

Tissue concentrations were calculated by dividing the amount recovered from a tissue sample by the weight of the tissue sample. The total amount recovered from each animal was the product of the specific organ concentration and the individual organ weight. The sum of all tissue weights in each animal approximated the total body weight minus the total weight of any GI contents and urine.

RESULTS

Single-Dose Pharmacokinetics of Methicillin—Following single bolus doses of methicillin, serum concentrations declined in a biexponential fashion, as shown for three representative rabbits in Fig. 2. Such profiles were fitted to Eq. 4 by nonlinear least-squares regression (14). The SHAM properties were then inserted into Eqs. 7–17 to obtain the pharmacokinetic parameters describing clearance and distribution in the 15 rabbits given single doses. These data are given in rank order of dose in Table I, and show that the average serum concentration remains proportional to dose with increasing doses, while the plasma clearance remained essentially constant, averaging 0.60 ± 0.15 L/h/kg. The terminal half-life averaged 27 ± 2 min in the rabbits. The other parameters that remained constant over this dosage range were V_c, which averaged 0.20 ± 0.03 L/kg, and CL_{21}, which averaged 1.86 ± 0.60 L/h/kg. The t, Vd_{ss}, and CL_{12} values varied with dose. Vd_{ss} decreased by approximately twofold as the dose covered a 10-fold range. The change in t with dose was a direct result of the Vd_{ss}/CL ratio, as the plasma clearance remained unchanged with increasing doses. The distributional clearances (CL_{12}) listed in Table I exhibited a fourfold range (0.10–0.35 L/kg/h) with increasing doses of methicillin.

[1] A Hemoccult pad was placed in the abdominal cavity next to the collection tube or filter disk.

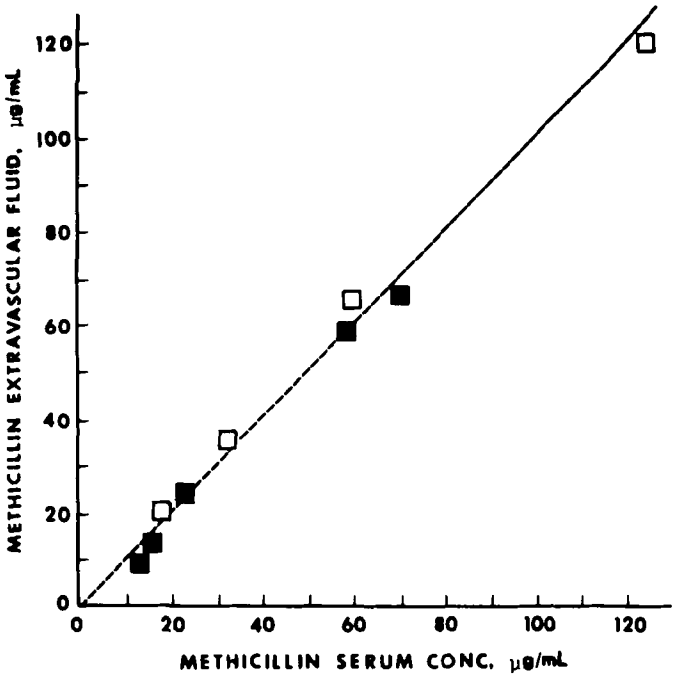

Figure 3—*Simultaneous steady-state concentrations of methicillin in serum and extravascular fluids: Key: (■) tissue chamber fluid; (□) peritoneal fluid.*

To assess the possibility of protein binding changes altering the distribution volume, we measured protein binding by equilibrium dialysis on serum samples over a 20-fold range of serum concentrations. The binding of methicillin to serum proteins averaged 17 ± 2%.

Methicillin Pharmacokinetics after Continuous Infusions—Methicillin was infused into 11 different rabbits for 6–10 h. The infused doses, clearances, volumes of distribution, total body methicillin content (X_B^{ss}), and serum concentrations measured at steady state are listed in Table II for each of these rabbits. The C^{ss} values were proportional to the infusion rate, yielding relatively constant CL values which averaged 0.86 ± 0.19 L/kg/h. These values were in good agreement with the single dose CL values of Table I. As was observed in the single-dose rabbits, Vd_{ss} steadily declined as doses and steady-state serum concentrations increased.

Steady-State Extravascular Fluid Distribution—Table III gives the steady-state serum drug concentrations for all 11 rabbits, ranging from 13.0 to 125.0 μg/mL. As serum concentrations increased as a result of the increasing dosing rates, a proportional rise was noted in the extravascular fluid concentrations, *i.e.*, both the tissue chamber and peritoneal fluid. The data indicate complete and dose-independent penetration of methicillin into extravascular fluids, as shown by the identity line in Fig. 3.

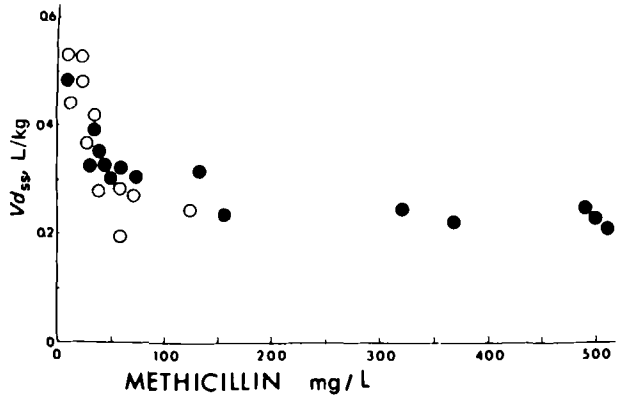

Figure 4—*Steady-state volume of distribution following a single dose (●) and constant infusion (○) of methicillin in relation to time average (C_{av}) and steady-state (C^{ss}) serum drug concentrations.*

Table III—Steady-State Serum, Extravascular Fluid, and Nonexcretory Tissue Concentrations Following Constant Infusion

Rabbit	C^{ss}, μg/mL[a]	Conc. in Tissue Chamber[b] or Peritoneal Fluid[c], μg/mL	Steady-State Tissue Conc., μg/g[c]			
			Heart	Lung	Liver	Skeletal Muscle
16	13.0 ± 1.5	11.0	5.0	4.8	5.0	4.4
17	15.0 ± 1.2	13.8	7.5	4.6	6.3	7.5
18	17.4 ± 1.8	20.0[d]	8.8	8.9	7.8	8.9
19	22.5 ± 1.3	24.0	23.0	3.9	9.7	7.1
20	30.7 ± 2.1	—[e]	8.2	6.5	8.8	11.0
21	34.5 ± 2.7	32.0[d]	10.7	10.0	16.6	11.2
22	38.5 ± 1.3	—[e]	9.0	7.7	8.2	10.2
23	58.9 ± 2.4	65.0[d]	23.0	34.6	30.4	6.7
24	60.0 ± 3.0	58.0	10.0	9.6	14.0	13.5
25	71.0 ± 2.6	67.0	10.4	8.8	11.3	15.8
26	125.0 ± 6.3	120.0[d]	31.0	35.0	35.0	24.0

[a] Steady-state methicillin serum concentration verified by measurement every 30 min over the 6-10-h infusion period (values ± *SD*). [b] Steady-state methicillin concentration measured in fluid obtained from a subcutaneously implanted perforated plastic catheter. [c] Methicillin concentrations measured at the time of sacrifice, immediately following the infusion. [d] Peritoneal fluid samples. [e] Not analyzed because sample contained occult blood.

The methicillin content of the bile was <5% of the infused dose, but represented only the bile present in the gallbladder at the time of sacrifice. The volume of bile that entered the GI tract during the infusion period was not assessed.

Urinary Excretion—Urine collected over the first 24 h from animals receiving single doses of methicillin contained 80 ± 2% of the administered dose. In animals infused to steady state and sacrificed, urine was collected from the intact bladder at the end of infusion. Greater than 85% of the administered dose could be accounted for in the serum, tissue, and urine of this group of rabbits. The percentage of the total dose that appeared in the urine at the time of sacrifice consistently increased as the cumulative dose infused increased. At the lowest infusion dose, 67% of the dose appeared in the urine, while at the highest dose, 96% of the total dose appeared in the urine. Despite this finding, the total body clearance of methicillin in these two rabbits was similar: 0.67 and 0.69 L/kg/h.

In vitro experiments revealed that methicillin was not completely stable in rabbit urine. The half-life for methicillin degradation in rabbit urine maintained at 39°C averaged 31 ± 4 h. If a degradation rate constant is incorporated into the urine recovery and the total amount of methicillin excreted in the bile estimated, essentially all of the total infused dose can be accounted for in the rabbits sacrificed at steady state.

Steady-State Tissue Penetration—The steady-state concentrations of methicillin in representative nonexcretory tissue are listed in Table III along with simultaneous C^{ss} and extravascular fluid concentrations. Unlike steady-state serum and extravascular concentrations, steady-state concentrations in nonexcretory tissue did not increase proportionally with increases in infusion rate. Steady-state tissue concentrations seemed to reach an apparent plateau as steady-state serum concentrations exceeded 25–30 μg/mL. Furthermore, the total amount in the body at the time of sacrifice (X_B^{ss}) appeared to approach a maximum value as infusion rates increased. Steady-state kidney concentrations of methicillin were generally 10-fold greater than concentrations in nonexcretory tissue, and the plateau of concentrations with increased doses was less marked. However, true renal tissue concentrations could not be discerned because we were also measuring drug in retained urine in the kidney samples.

Consistent with the individual values in tissue, the total amount of methicillin recovered from each rabbit at steady state also failed to increase proportionally to increased infusion doses, as shown in Table III. The steady-state volume of distribution of methicillin varied over twofold, but values consistently diminished as steady-state concentrations were increased with increasing dosing rates.

Nonlinear Steady-State Volume of Distribution—The nonlinear relationship between Vd_{ss} and methicillin steady-state serum concentrations can be evaluated directly from the data in Table II. The single-dose studies in Table I yield time-average Vd_{ss} values which can be assessed only at the time-average serum concentration (C_{av}). Figure 4 depicts all methicillin Vd_{ss} values in relation to either C_{av} or C^{ss}; these data are consistent with a single nonlinear curve. It should be noted that the largest C_{av} range produced Vd_{ss} values which approach a limiting value of ~0.20 L/kg, similar to the mean central compartment volume of distribution.

The decline in both Vd_{ss} and CL_{12} with increasing C^{ss} suggested that limiting tissue uptake was a common factor. Equation 26 was employed to characterize the data of Fig. 4 in the following manner. The NONLIN computer program was used to fit individual Vd_{ss} values as a function of actual C_{av} from each animal dosed by rapid intravenous bolus doses. Individual values of V_c were available, and specific values of V_T were then directly calculated for each animal using Eq. 15. This left three unknown parameters, T_{max}, K_m, and CL_{21}. These were generated using least-squares regression. Initial estimates were obtained as described in the *Theoretical Section.*

The mean (± *SD*) least-squares values which described the nonlinear extravascular penetration of methicillin in the rabbit following single intravenous bolus doses were: T_{max} = 9.79 ± 4.3 mg/kg/h; K_m = 17.2 ± 7.0 μg/mL; and CL_{21} = 1.02 ± 0.6 L/kg/h. To test the ability of this model to predict distribution at steady-state from single-dose data, the parameter estimates from the single-dose data were used to calculate the Vd_{ss} in animals infused to steady state, using Eq. 26. As shown in Fig. 5, these calculated values were in good agreement with the measured values in all rabbits infused to steady state.

Multiple Single Doses—Additional studies were performed using a wider range of single doses (15–500 mg/kg) in crossover fashion to further examine the linearity of the disposition of methicillin. The *CL* from Eq. 8 and Vd_{ss} from Eq. 9 following these doses of methicillin in each of five rabbits are shown in Table IV. The Vd_{ss} following the 15-mg/kg dose was significantly larger than the Vd_{ss} following the 50-mg/kg dose. The Vd_{ss} changes are in agreement with those predicted in previous rabbits given large doses of methicillin either by rapid bolus or continuous infusion. The Vd_{ss} following the 500-mg/kg doses approximates the total extracellular fluid volume of 0.17 L/kg in New Zealand White rabbits (15).

The 500-mg/kg methicillin dose yielded a lower clearance compared with those following the lower doses. The *CL* values from the lower doses were similar. These data indicate that the assumption of linearity in total methicillin clearance is tenable only over a limited dose and concentration range.

DISCUSSION

Disposition in Rabbits—From measurements of the drug in serum and urine, it appears that methicillin is primarily cleared by the kidney and excreted in the urine of the rabbit. This is in agreement with other reports of methicillin pharmacokinetics in rabbits (16) and is also consistent with human studies (17). The renal clearance of methicillin, like other penicillins, has been attributed to both glomerular filtration as well as active tubular secretion (18). Concomitant administration of organic acids such as *p*-aminohippuric acid and probenecid have shown to competitively inhibit the active secretion process (19, 20). At sufficiently high methicillin concentrations, renal clearance also becomes nonlinear, as was observed after single 500-mg/kg doses in these studies (Table IV). The model assumptions only apply to the region of linear clearance.

There was a consistent, near-total recovery of the infused dose of methicillin from tissue, serum, and urine in all animals dosed to steady state, regardless of the total dosage. Furthermore, the unrecovered drug can be accounted for by the instability of methicillin in rabbit urine and incomplete collection of bile. Thus, the pharmacokinetic model can be applied in a setting where mass balance is essentialy complete without uncertainties related to incomplete tissue extraction or analytical difficulties. The pharmacokinetic characterization of serum concentration *versus* time profiles yielding nonlinear tissue distribution properties was directly confirmed by analysis of actual tissue drug uptake. This diminishes the need for speculative inferences regarding the physiological relevance of the pharmacokinetic analysis of only serum concentrations.

Tissue Distribution—The distribution of methicillin into extravascular spaces can be described by two processes. Methicillin distributed freely and rapidly between serum and extravascular fluids since peritoneal fluid and tissue chamber fluid concentrations are in good agreement with serum concentra-

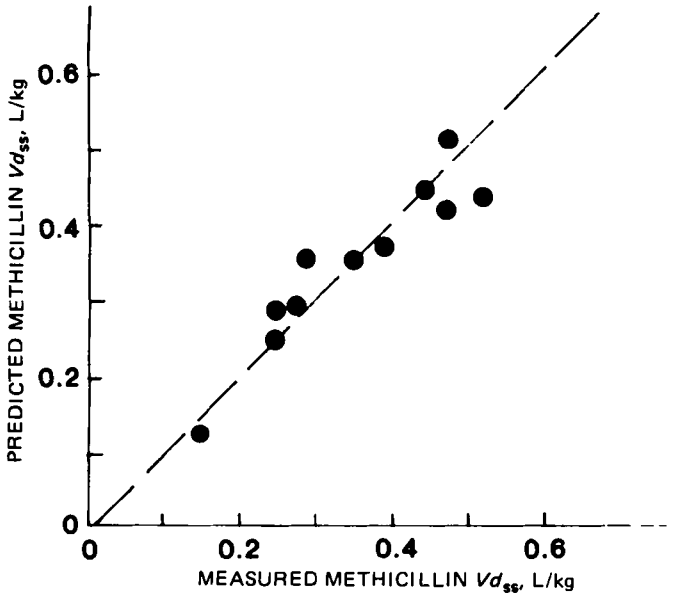

Figure 5- *Agreement between predicted* Vd_{ss} *(Eq. 26) using the* V_c, V_T, T_{max}, K_m, *and* CL_{21} *values obtained from single-dose studies and measured* Vd_{ss} *based on recovery of drug from body tissue.*

tions, even following single doses. This process is a simple linear relationship. Similar findings with other penicillins have been reported in animals (21) and in humans (22). In contrast, the intracellular distribution of methicillin appears to be governed by a different process. A plateauing of steady-state tissue concentrations occurred as C^{ss} exceeded 20–25 μg/mL. Linear uptake occurs at low serum concentrations, but saturation begins to occur as the K_m (17 μg/mL) is exceeded. Each tissue analyzed contains cells, interstitial fluid, and trapped blood. Interstitial fluids are in rapid equilibrium with drug in plasma (Fig. 3). When the conglomerate of tissue and interstitial fluid is homogenized for assay, measured concentrations of methicillin continue to rise slightly as C^{ss} increases, but not to a proportional degree. Apparently, interstitial fluid concentrations continue to parallel serum, while true tissue concentrations reach a limiting value. Similar tissue penetration data using ampicillin have recently been reported by Cars and Ogren (23). Skeletal muscle concentrations of ampicillin were substantially lower than serum concentrations, but concentrations declined at a similar rate from both tissue and serum. They, like we, suggest that ampicillin concentrations in interstitial fluid are considerably higher than whole tissue concentrations.

The capacity-limited nature of methicillin tissue distribution in rabbits was best described by a pharmacokinetic model incorporating a linear systemic clearance and a Michaelis-Menten-type, nonlinear distributional clearance. The unique pharmacokinetic manifestation of the nonlinear distributional clearance is that the Vd_{ss} changes as serum concentrations or doses change. At high serum concentrations, Vd_{ss} approaches its minimal value, which is V_c. This occurs following both rapid intravenous bolus or steady-state infusion of the drug. The volume of the central compartment was consistent for all rabbits and was independent of dose. The central volume takes on physiological significance because it is slightly larger than the value for extracellular fluid volume in New Zealand White rabbits (15). The excellent agreement between measured concentrations of methicillin in serum and extravascular fluids confirms that V_c is comprised of the plasma and interstitial volumes. The tissue volume V_T also retains physiological significance because it is simply the summation of the tissue weights excluding the weight of blood and interstitial fluids.

This is not the first observation of an apparent capacity-limited process with penicillins. Active processes for tubular secretion have been known. The active tubular secretion of penicillins can be saturated (24) and inhibited by *p*-aminohippuric acid (19). Saturable renal tubular processes have also been observed following the administration of mezlocillin (25), cephapirin (3), and cephaloridine (3) to human volunteers. This also appears to occur for methicillin at very high doses.

Regarding tissue uptake, Bergholtz *et al.* (26) reported that probenecid, an inhibitor of the active secretion of penicillin, can affect skeletal muscle concentrations of penicillin. Pappenheimer *et al.* reported an active transport process for the movement of organic acids from CSF to plasma (27) which has been shown to be operative for benzylpenicillin (6). There are numerous reports of penicillin neurotoxicity following massive dosing, presumably overwhelming the central nervous system active transport system for penicillin

Table IV—Methicillin Clearance and Vd_{ss} in Five Rabbits, Each Given Three Doses of Methicillin in Randomized Order

	Clearance, L/h/kg			Vd_{ss}, L/kg		
Rabbit	15 mg/kg	50 mg/kg	500 mg/kg	15 mg/kg	50 mg/kg	500 mg/kg
27	0.97	0.70	0.55	0.42	0.27	0.19
28	0.88	0.78	0.73	0.35	0.20	0.22
29	1.50	1.30	0.90	0.49	0.21	0.25
30	1.00	1.00	0.60	0.40	0.25	0.19
31	1.10	1.10	0.60	0.36	0.29	0.19
Mean	1.09	0.97	0.67	0.40	0.24	0.20
± *SD*	0.24	0.28	0.14	0.05	0.03	0.02
		$p < 0.05$		$p < 0.05$		

removal (28, 29). Studies by Fishman (30) suggest that probenecid may cause CNS accumulation of penicillin.

Similar active transport systems have been proposed to explain the concentration dependence of ampicillin excretion into bile (31). Recent data obtained from rats suggest that the absorption of amino penicillins is best described by Michaelis-Menten kinetics and postulate that similar saturable absorption processes govern cephalexin and cephradine absorption (5).

In addition to concentration dependence in renal and biliary secretion and GI absorption, another recently described concentration-dependent process with β-lactam antibiotics occurs with protein binding. The third generation caphalosporin, ceftriaxone, is a particularly good example of this phenomenon, as the saturation of binding occurs at plasma concentrations in the usual therapeutic range (32).

Concentration-dependent tissue distribution has not been described for β-lactam antibiotics. The data presented here for methicillin suggest that essentially all nonexcretory tissues can be involved in this process, and establish a limit to achievable "tissue" concentrations for these antibiotics. Such an observation, if confirmed for other β-lactam antibiotics, has clinical relevance to the treatment of infection. However, not only do other drugs need study for similar concentration dependence, but also it is not yet possible for the data presented to differentiate whether this phenomenon is caused by capacity limits in binding to tissue proteins or a saturable cellular uptake process. It does appear from these data that whichever the underlying mechanism, the process limits the concentrations of methicillin that can be realistically achieved in normal tissue.

Transit Times—An innovative approach was evolved to relate a single-dose disposition of methicillin to true steady-state conditions. The analysis of single-dose kinetics based on the SHAM characteristics is valid for linear conditions, but entails the generation of dose and time-average pharmacokinetic parameters in the nonlinear dosage range. In the latter case, these time-average parameters ought to directly apply to steady-state conditions only at an equivalent time-average substrate concentration. This was confirmed experimentally for Vd_{ss} (Fig. 4, Table IV) and by the dual characterization of single-dose and steady-state data with a single nonlinear function (Eq. 26). Other uses of transit-time analysis have been reviewed recently (33).

APPENDIX: GLOSSARY

Concentrations

C	Serum or plasma concentration
C_T	Mean tissue concentration
C^{ss}	Steady-state serum concentration
C_i	Intercepts of C_p *versus* time curve
C_{av}	Time-average serum concentration
K_m	Michaelis-Menten constant for transport

Time

t	Experimental time
$\bar{t}$	Mean transit time

Slopes

λ_i	Slope of C_p *versus* time curve

Integrals

AUC	Area of C_p *versus* time curves
AUMC	Area of $t \cdot C_p$ *versus* time curve (moment)

Volumes, Weights

V_c	Volume of plasma and interstitial fluid
Vd_{ss}	Steady-state volume of distribution
TBW_t	Total body weight
V_T	Cellular tissue volume
V_{Ti}	Individual tissue weights

Clearances

CL	Systemic plasma clearance

CL_{12}	Clearance from plasma to cell water = $f(T_{max},K_m)$
CL_{21}	Clearance from cell water to plasma
Amounts	
D_0	Dose
X_B^{ss}	Amount in body at steady-state
Rates	
k_0	Zero-order infusion rate
T_{max}	Maximum cellular transport rate
Ratios	
K_d	Tissue-plasma partition coefficient
K_{pi}	Individual tissue-plasma partition coefficients

REFERENCES

(1) G. Levy, in "Importance of Fundamental Principles in Drug Evaluation," D. H. Tedeschi and R. E. Tedeschi, Eds., Raven, New York, N.Y., 1968, pp. 141-171.

(2) I. M. Weiner and G. H. Mudge, *Am. J. Med.*, **36**, 743 (1964).

(3) A. Arvidson, O. Borga, and G. Alvan, *Clin. Pharmacol. Ther.*, **25**, 870 (1979).

(4) S. K. Lin, A. A. Moss, and S. Riegelman, *J. Pharm. Sci.*, **66**, 1670 (1977).

(5) A. Tsuji, E. Nakashima, I. Kagami, T. Asano, and R. Yamana, *J. Pharm. Pharmacol.*, **30**, 508 (1978).

(6) R. L. Dixson, E. S. Owens, and D. P. Rall, *J. Pharm. Sci.*, **58**, 1106 (1969).

(7) W. J. Jusko and M. Gretch, *Drug Metab. Rev.* **5**, 43 (1976).

(8) A. R. DiSanto and J. G. Wagner, *J. Pharm. Sci.*, **61**, 1040 (1972).

(9) W. J. Jusko and J. Q. Rose, in "Frontiers in Therapeutic Drug Monitoring," G. Togoni, R. Latini, and W. J. Jusko, Eds., Raven, New York, N.Y., 1980, pp. 153-161.

(10) N. A. Lassen and W. Perl, "Tracer Kinetic Methods in Medical Physiology," Raven, New York, N.Y., 1979.

(11) L. Z. Benet and R. L. Galeazzi, *J. Pharm. Sci.*, **68**, 1071 (1979).

(12) F. W. Kavanaugh, *Pharm. Technol.*, **63**, 1459 (1974).

(13) J. J. Schentag, W. J. Jusko, J. W. Vance, E. Abrutyn, M. DeLattre, and M. Gerbracht, *J. Pharmacokinet. Biopharm.*, **5**, 559 (1977).

(14) C. M. Metzler, G. L. Elfring, and A. J. McEwen, *Biometrics*, **30**, 562 (1974).

(15) P. Altman and D. Dittmer, "Biology Data Book," 2nd ed., Vol. III, Federation of American Societies for Experimental Biology, Bethesda, Md., 1974, p. 1990.

(16) J. Carrizosa, W. Kobasa, and D. Kaye, *Antimicrob. Agents Chemother.*, **15**, 735 (1979).

(17) C. Kunin, *Clin. Pharmacol. Ther.*, **7**, 166 (1966).

(18) A. G. Gilman, L. S. Goodman, and A. Gilman, "The Pharmacological Basis of Therapeutics," 6th ed., Macmillan, New York, N.Y., 1980, p. 1136.

(19) K. Beyer, F. Woodward, L. Peters, W. Verwey, and P. Mattis, *Science*, **100**, 107 (1944).

(20) H. Eagle and E. Neuman, *J. Exp. Med.*, **25**, 903 (1947).

(21) M. Barza and L. Weinstein, *J. Infect. Dis.*, **129**, 59 (1974).

(22) J. Tan, A. Trott, J. Phair, and C. Watanakunakorn, *J. Infect. Dis.*, **126**, 492 (1972).

(23) O. Cars and S. Ogren, *J. Antimicrob. Ther.*, **6**, 408 (1980).

(24) T. Bergan and B. Oydvin, *Chemotherapy*, **20**, 263 (1974).

(25) A. Mangione, F. D. Boudinot, R. W. Schultz, and W. J. Jusko, *Antimicrob. Agents Chemother.*, **21**, 428 (1982).

(26) H. Bergholtz, R. R. Erttmann, and K. Damm, *Experentia*, **36**, 333 (1980).

(27) J. Pappenheimer, S. Heisey, and E. Jordan, *Am. J. Physiol.*, **200**, 1 (1961).

(28) K. Seamans, P. Gloor, R. Dobell, and J. Wyant, *N. Engl. J. Med.*, **278**, 861 (1968).

(29) P. New and C. Wells, *Neurology*, **15**, 1053 (1965).

(30) R. Fishman. *Arch. Neurol.*, **15**, 113 (1966).

(31) J. Kampman, F. Lindahl, J. Hansen, and K. Siersbaek-Nielsen, *Br. J. Pharmacol.*, **47**, 782 (1973).

(32) K. Stoeckel, P. J. McNamara, R. Brandt, H. Plozza-Nottebrock, and W. H. Ziegler, *Clin. Pharmacol. Ther.*, **29**, 650 (1981).

(33) W. J. Jusko, in "Applied Pharmacokinetics," W. Evans, J. J. Schentag, and W. J. Jusko, Eds., Applied Therapeutics, Inc., San Francisco, Calif., 1980, p. 639-680.

Pharmacokinetics of Nitroglycerin after Parenteral and Oral Dosing in the Rat

HO-LEUNG FUNG ˣ, H. OGATA *, A. KAMIYA ‡, and G. A. MAIER §

Received May 17, 1982, from the *Department of Pharmaceutics, School of Pharmacy, State University of New York at Buffalo, Amherst, NY 14260.* Accepted for publication June 23, 1983. Present addresses: *National Institute of Hygienic Sciences, Tokyo, Japan, ‡Kyoto University Hospital, Kyoto, Japan, and § Schering Corporation, Bloomfield, NJ 07003.

Abstract □ The pharmacokinetics of nitroglycerin was characterized in detail using venous plasma after different intravenous bolus doses (0.15-2.48 mg/kg), intra-arterial infusion (8.2 μg/min over 5 h), and oral doses (7-100 mg/kg). Venous plasma clearance was found to be ~650 mL/kg and was independent of the intravenous or intra-arterial dose. This confirmed earlier reports that the venous plasma clearance of nitroglycerin in rats exceeded the value of normal cardiac output. A terminal half-life of ~15 min was observed after high intravenous bolus doses of nitroglycerin. This slow disappearance phase was likely rate limited by redistribution of drug back into the plasma. The bioavailability of oral nitroglycerin (F) showed an apparent Michaelis-Menten dependency on dose. F was <5% at doses <20 mg/kg, but increased to a plateau of ~20% from 50-100 mg/kg. First-pass metabolism of nitroglycerin is thus apparently controlled by at least two systems (sites or enzymes). Coadministration of mannitol hexanitrate, a potential competitive inhibitor of first-pass metabolism, did not increase F.

Keyphrases □ Pharmacokinetics—nitroglycerin, parenteral and oral dosing, rats □ Nitroglycerin—pharmacokinetics, parenteral and oral dosing, rats

Interest in the clinical use of intravenous nitroglycerin has intensified in recent years because of its demonstrated efficacy in treating the resultant manifestations of myocardial infarction, congestive heart failure, and unstable angina. Several reports (1-3) have shown that intravenous infusion of nitroglycerin can appreciably decrease cardiac work load and relieve the increase in left ventricular and diastolic pressure secondary to congestive heart failure or myocardial infarction (2).

Despite the increasing popularity of the use of intravenous nitroglycerin in therapy, very little is known about the pharmacokinetic behavior of this potent drug. There are indications

0022-3549/84/0700-0873$01.00/0